

1993-14

**BEDROCK GEOLOGIC CONTROLS ON RADON ABUNDANCE IN  
DOMESTIC WELL WATER, CONIFER, COLORADO**

David Frishman, W. C. Day, P. F. Folger, R. B. Wanty, and P. H. Briggs  
U.S. Geological Survey  
Denver, CO

Eileen Poeter  
Colorado School of Mines  
Golden, CO

**ABSTRACT**

Radon in ground water used for domestic supply can contribute significantly to radon concentrations in indoor air. Our integrated studies of bedrock geology, bedrock and well-water chemistry, geohydrology, and downhole geophysics have delimited some of the features that can exert broad regional as well as local control on radon abundance in well water from crystalline rock aquifers. Local, small-scale features such as inhomogeneities in the distribution and mineralogical residence of uranium in the bedrock and on fracture surfaces exert the strongest control on partitioning of radon between the bedrock aquifer and its entrained ground water. Detailed geologic mapping (meter-scale) has outlined zones in the granite bedrock that are enriched in uranium by an order of magnitude. Alpha-track mapping of thin sections (millimeter-scale) demonstrates that iron-oxide coatings on fracture surfaces are enriched in alpha-emitting elements that may be contributing radon to the well water. Although bedrock composition determines the general abundance of radon in ground water, the local features control radon concentration in any given well.

**INTRODUCTION**

The main goals of this ongoing study are to characterize and understand the natural geological and hydrochemical processes governing the mobility of  $^{222}\text{Rn}$  in ground water and to determine the extent to which  $^{222}\text{Rn}$  in a water supply may contribute to  $^{222}\text{Rn}$  in indoor air. This paper will mention some of our results concerning the contribution of water-borne  $^{222}\text{Rn}$  to indoor air, but it will concentrate on the geological aspects of our investigations. The hydrochemical and hydrologic aspects of the investigations will not be discussed.

**GEOLOGY**

The study area is located near Conifer, Colorado, in the foothills southwest of Denver (Fig. 1). It is underlain by an Early Proterozoic migmatite terrane that was extensively invaded by granitic plutons of the Middle Proterozoic Silver Plume Granite, which are part of the Berthoud Plutonic Suite, and the Middle Proterozoic Pikes Peak Granite (Bryant and others, 1981).

The migmatitic rocks, about 1,700 million years old (Ma), are the oldest bedrock unit in the study area. This rock (units Xb, Xm, and Xma; Fig. 1) comprises a number of rock types including older biotite schist, amphibolite, biotite gneiss, and minor quartzite and calc-silicate gneiss (the paleosome) containing numerous layers, pods, and lenses of at least two generations of younger granitic gneiss and granite (the neosome). These rocks were strongly deformed and metamorphosed in Early Proterozoic time. A brief summary of the geology of this terrane, as well as many additional references, is contained in Condie (1992).

The migmatitic rocks are a deformed layered sequence and the bulk composition of the individual layers differs widely at the scale of a centimeter to a few meters. However, the effect of these short-range differences in bedrock chemistry on ground-water chemical composition are probably averaged to some degree as the ground water

flows through the rock. Table 1 lists the average chemical compositions and standard deviations for samples of the granitic neosome (columns one and two) and the mafic paleosome (columns three and four). Although the bulk composition is quite varied, the average uranium concentration is low (about 3 parts per million (ppm)). However, some samples are relatively enriched in uranium--one sample from a brittle-fault zone contained nearly 6 ppm uranium.

The Middle Proterozoic Silver Plume Granite (unit Ysp, Fig. 1) is about 1,400 Ma (see discussion of the Berthoud Plutonic Suite (Middle Proterozoic) and references in Aleinikoff and others, 1993). It intrudes the migmatitic rocks in the eastern part of the study area, but it will not be considered further in this paper.

The Middle Proterozoic Pikes Peak Granite, about 1,100 Ma, is the most areally extensive rock unit in the study area. The Pikes Peak Granite exposed in the study area (unit Ypp, Fig. 1) is part of the much larger Pikes Peak batholith, which occupies more than 3,000 km<sup>2</sup> in central Colorado southwest of Denver and west of Colorado Springs (Barker and others, 1975). Within the study area, the Pikes Peak Granite is dominantly a pinkish-gray, coarse-grained, equigranular biotite-hornblende granite. It is relatively enriched in fluorine as well as in the rare-earth elements and uranium. Uranium concentrations in the Pikes Peak Granite average nearly 5 ppm and fluorine concentrations are slightly less than 0.2 weight percent (Table 1, columns 5 and 6). The high fluorine concentrations in the Pikes Peak Granite are reflected in the ground-water chemistry (Wanty and others, 1992).

Regionally extensive shear zones cut across all of the bedrock units. These shear zones are dominantly northwest trending (Fig. 1) and are zones of intense faulting and associated brittle deformation. The bedrock within these zones shows evidence of iron-oxide alteration. The zones are deeply weathered and poorly exposed, rendering sampling difficult. However, the limited number of samples from the shear zones record major chemical differences compared to the original bedrock. Samples from shear zones where they cut across the migmatite have major-element compositions intermediate to those of the neosome and paleosome component of the migmatite. However, as noted above, one sample from a shear zone in the migmatite has a higher uranium content than the original rock. Uranium enrichment also has been found in a sample from a shear zone in the Pikes Peak Granite. This sample (Fig. 1, sample CO-91-38) contains nearly an order of magnitude more uranium (45 ppm) than the average Pikes Peak Granite (4.8 ppm). Additionally, an alpha-track map of a polished thin section prepared from this sample indicates that the elements that emit alpha particles in this sample are concentrated along iron-stained fractures (Fig. 2), sites from which uranium could presumably be more readily leached than if the uranium were tightly bound in a crystalline mineral like zircon. These samples indicate that redistribution and enrichment of uranium has occurred in the shear zones, at least on a local scale. These brittle shear zones may be an important source for <sup>222</sup>Rn in ground water. This result is in general agreement with previous studies of ductile shear zones in the eastern U.S. (Gundersen, 1989).

#### DETAILED RADIOMETRIC AND GEOLOGIC MAPPING OF THE WOODSIDE SUBDIVISION

Our results indicate a broad correlation between bedrock type and ground-water composition. Domestic wells completed in the Pikes Peak Granite are enriched in radon relative to those in the metamorphic terrane. Samples of Pikes Peak Granite average about 5 ppm uranium, with well water from the Pikes Peak Granite containing an average of  $4.1 \times 10^5$  becquerel of radon per cubic meter ( $\text{Bq m}^{-3}$  ( $1.1 \times 10^4$  picocuries per liter ( $\text{pCi l}^{-1}$ ))). Samples from the metamorphic terrane average about 3 ppm uranium and associated well water is correspondingly lower in radon, having an average of  $1.48 \times 10^5 \text{ Bq m}^{-3}$  ( $4 \times 10^3 \text{ pCi l}^{-1}$ ) radon. However, the range of radon concentrations for both terranes is quite large. Radon in wells within the Pikes Peak Granite ranges from  $7.4 \times 10^4$  to  $8.9 \times 10^5 \text{ Bq m}^{-3}$  ( $2 \times 10^3$  to  $2.4 \times 10^4 \text{ pCi l}^{-1}$ ), whereas within the metamorphic terrane it ranges from  $3.4 \times 10^4$  to  $4.8 \times 10^5 \text{ Bq m}^{-3}$  ( $1 \times 10^3$  to  $1.3 \times 10^4 \text{ pCi l}^{-1}$ ; Fig. 3). However, adjacent domestic water wells that are within the same bedrock unit but are not within or near known shear zones can also show a wide variation in <sup>222</sup>Rn content.

One area in which the uranium concentrations are highly varied is the Woodside subdivision in the northwest part of the study area north of Pine Junction, Colorado (Fig. 1). The area is underlain by what superficially seems to be homogeneous Pikes Peak Granite. However, water samples from wells in the subdivision exhibit a wide and unpredictable range in <sup>222</sup>Rn concentrations from  $7.4 \times 10^4$  to  $7.4 \times 10^5 \text{ Bq m}^{-3}$  ( $2 \times 10^3$  to  $2 \times 10^4 \text{ pCi l}^{-1}$ ) between wells that are only 50 to 150 m apart.

Detailed geologic mapping and radiometric surveys were undertaken on a single outcrop to determine the cause of the widely divergent  $^{222}\text{Rn}$  concentrations in closely spaced water wells. A small outcrop in the Woodside subdivision was mapped at a scale of 1:24 (one inch = two feet). We laid out and staked down a grid of reference strings on the outcrop on 3.05 m (ten ft) centers. Chalk lines were snapped onto the rock at 0.61 m (two ft) intervals between the reference strings, and this two-foot grid was used as a reference both for the geologic map and the gamma-ray survey. It was felt that a geologic map of this well-exposed outcrop could serve as a good analog for the geologic conditions existing in the nearby water wells.

The outcrop is composed of coarse-grained biotite-hornblende granite, a phase typical of some portions of the Pikes Peak Granite (fayalite-free granite of Barker and others, 1975). This dominant lithology is cut by aplite and pegmatite dikes (Fig. 4). However, there are subtle variations in the texture of the Pikes Peak Granite marked by small (<3m wide) zones that are medium-grained biotite leucogranite. Normally these textural variations would be overlooked during a regional survey. However, these zones have remarkably high equivalent uranium and thorium (eU and eTh) contents (Fig. 4). Measured eU abundances are as much as a factor of 5 (25 ppm) greater than the average for the Pikes Peak Granite (Table 1, column 5) in the medium-grained areas. In addition, there are zones relatively enriched (by a factor of 2) in eU that are underlain by and adjacent to the aplite dikes (Fig. 4). Aplites have higher total gamma counts (as we have also observed from some well logs), but these gamma counts appear to be mostly from thorium, and therefore will not contribute much indoor radon.

Radiometric surveys were conducted with both a hand-held Mt. Sopris Instrument Co. model SC-132\* gamma-ray scintillometer and a larger Scintrex model GAD-6 gamma-ray spectrometer. The Scintrex spectrometer used a model GSP-3 sodium-iodide scintillation detector with a volume of 348 cm<sup>3</sup>. Data were collected at each of the 512 nodes of the two foot grid with the total-count scintillometer (512 points) and at 150 selected nodes with the spectrometer. With the spectrometer, counts were accumulated for 100 seconds at gamma-ray energy levels corresponding to the  $^{214}\text{Bi}$ ,  $^{208}\text{Tl}$ , and  $^{40}\text{K}$  peaks. From these data, values were calculated for eU, eTh, and potassium--it is these calculated values for eU that were used to produce the contour map shown in Fig. 4.

Equivalent uranium abundances range from less than two to more than 25 ppm, averaging about 6 ppm. The average abundance as determined by the gamma-ray spectrometer is close to the average uranium content of the 10 samples of Pikes Peak Granite analyzed to date (average value of 4.8 ppm; Table 1, column 5). Therefore, the variations in uranium abundance measured within this small outcrop are probably real. The highest eU abundance found coincides with a zone of very high thorium (eTh = 380 ppm). Petrographic examination and semi-quantitative analysis using a scanning electron microscope (SEM) of the first few thin sections prepared from the Woodside outcrop samples indicates the presence of the minerals allanite and thorite. Allanite usually contains tens of ppm to a few percent uranium, though perhaps not in this association, and thorite, nominally  $\text{ThSiO}_4$ , invariably contains some uranium substituted for thorium. Owing to interferences in the X-ray spectrum and limitations of the energy-dispersive X-ray detector, SEM analyses for uranium in the presence of large amounts of thorium require large numerical corrections for peak overlap. These analyses, therefore, are moderately equivocal, but preliminary results indicate that the Woodside thorites contain eight to ten weight percent  $\text{UO}_2$ .

The most important conclusion to be drawn from this detailed mapping is that even in areas underlain by ostensibly homogeneous granite, eU concentration can range widely. These large variations in uranium concentration should be expected to have a large local influence on  $^{222}\text{Rn}$  concentrations on ground water. Such large variations in uranium concentration observed on such a small scale suggests that caution must be exercised when making regional predictions of areas likely to have severe  $^{222}\text{Rn}$  problems.

## RADON IN WATER AND RADON IN AIR

---

\* Any use of trade, product, or firm names is for descriptive purposes only and does not imply endorsement by the U.S. Geological Survey. The portable field scintillometer portion of the Mt. Sopris Instrument Company is no longer in business. Scintrex is located at 4 Thorncliff Park Drive, Toronto, Ontario, Canada, M4H 1H1.

The question can still be asked, does  $^{222}\text{Rn}$  in well water contribute to  $^{222}\text{Rn}$  in indoor air? For this study we conducted a variety of tests for indoor radon on time scales ranging from 5 minutes to 4 months. In each case, our goal was to resolve the contribution of radon from the soil gas from that of the well water. Combined with a direct measurement of radon in the well water, this would allow us to determine the relative importance of well water as a contributor to indoor radon. Our results indicate that  $^{222}\text{Rn}$  in domestic well water can contribute significantly to  $^{222}\text{Rn}$  indoor air, but that this contribution is significant only if well water  $^{222}\text{Rn}$  is very high (hundreds of thousands of  $\text{Bq m}^{-3}$  or tens of thousands of  $\text{pCi l}^{-1}$ ) and the contribution is only measurable if it is not masked by high indoor  $^{222}\text{Rn}$  levels resulting from  $^{222}\text{Rn}$  contributed by the soil gas.

Short term measurements were performed using continuous-monitoring equipment manufactured by Pylon Electric Development Company<sup>†</sup>. The Pylon instrument records a cumulative count rate for radon decay over a preset counting period. These continuous monitors were installed in five houses for periods of 5 to 10 days; some houses were measured twice. During the time that continuous monitors were installed in the house, the residents were asked to keep a log of their water usage (showers, baths, washing-machine runs, etc.). If the water contributes significantly to indoor radon, a spike in the indoor radon concentration should be observed soon after each water-use event. The magnitude of that spike, compared to the radon concentration in well water, would then give an individual transfer coefficient for the airborne radon contribution from the water supply for that house.

In a number of the houses examined using this technique, the contribution of radon from the soil gas, as represented by the radon contribution of basement air, was so high that any water contribution was masked by diurnal or shorter-term variations. In one such case, a high-volume fan was connected to an exterior perimeter drain that had been installed around the foundation of the house at the time of construction. The results of this test are shown in Fig. 5. Before the fan was turned on, the continuous monitors were placed in the house and began measuring at 15-minute intervals. After four days, the homeowner turned on the fan, so that air would be drawn out from around the foundation. Within two hours, the basement air concentration dropped from  $>5,550 \text{ Bq m}^{-3}$  to  $<148 \text{ Bq m}^{-3}$  ( $>150 \text{ pCi l}^{-1}$  to  $<4 \text{ pCi l}^{-1}$ ). Similar precipitous decreases were observed on main level of the house. After the fan was turned on, spikes were still evident which corresponded exactly to the times at which water was used in the house, usually the washing machine. The well water serving this house contained about  $8.14 \times 10^5 \text{ Bq m}^{-3}$  ( $2.2 \times 10^4 \text{ pCi l}^{-1}$ ) of  $^{222}\text{Rn}$ . The spikes in radon concentration observed in the laundry room were up to  $1,850 \text{ Bq m}^{-3}$  ( $50 \text{ pCi l}^{-1}$ ). In the adjoining dining room, radon increased to more than  $370 \text{ Bq m}^{-3}$  ( $10 \text{ pCi l}^{-1}$ ). In both cases, the spike was rapidly attenuated; and background levels were observed again within four hours of the water use. No effect of water use was observed in the basement.

Further analysis of these data indicates that the transient spikes of radon from the water use contributes up to 20% of the average radon abundance in indoor air in the laundry room. Contributions were as much as  $274 \text{ Bq m}^{-3}$  ( $7.4 \text{ pCi l}^{-1}$ ) of  $^{222}\text{Rn}$  added to indoor air per day in the laundry room.

## CONCLUSION

Radon in ground water used for domestic supply can contribute significantly to radon concentrations in indoor air. Our integrated studies of bedrock geology, bedrock and well-water chemistry, geohydrology, and downhole geophysics have delimited some of the features that can exert broad regional as well as local control on radon abundance in well water in crystalline aquifers.

Local, small-scale features such, as inhomogeneities in the distribution and mineralogical residence of uranium in the bedrock, exert the strongest control on partitioning of radon between the bedrock aquifer and its entrained ground water. Detailed geologic mapping (meter-scale) in the Pikes Peak Granite has outlined uranium-enriched zones differentiated by an order of magnitude in uranium content (eU). Alpha-track mapping of rock thin section (millimeter-scale) demonstrates that iron-oxide coatings on fracture surfaces are enriched in alpha-emitting

---

<sup>†</sup> Any use of trade, product, or firm names is for descriptive purposes only and does not imply endorsement by the U.S. Geological Survey. Pylon Electric Development Co. is located at 147 Colonnade Road, Ottawa, Ontario, Canada K2E 7L9.

elements that may be contributing radon to the well water. Although bedrock composition determines the general abundance of radon in ground water, the local features control radon concentration in any given well.

### ACKNOWLEDGMENTS

Funding for this study was provided by the U.S. Geological Survey and by the U.S. Department of Energy under Interagency Agreement No. DE-AIO5-91ER61143. Philip Nyberg of the U.S. Environmental Protection Agency kindly lent us equipment to aid in some of the radon measurements described. Thoughtful and expedient reviews by F. A. Hills and R. R. Schumann are greatly appreciated. G.L. Hoffman aided with photography.

### REFERENCES

- Aleinikoff, J. N.: Reed, J. C.: DeWitt, E. The Mount Evans batholith in the Colorado Front Range: Revision of its age and reinterpretation of its structure. *Geological Society of America Bulletin* 105:791-806; 1993.
- Barker, F.: Wones, D. R.: Sharp, W. N.: Desborough, G.A. The Pikes Peak Batholith, Colorado Front Range, and a model for the origin of the gabbro-anorthosite-syenite-potassic granite suite. *Precambrian Research* 2:97-160; 1975.
- Bryant, B.: McGrew, L. W.: Wobus, R. A. Geologic map of the Denver 1° X 2° quadrangle, north-central Colorado. U.S. Geological Survey Miscellaneous Investigations Series Map I-1163: 1981.
- Condie, K. C. Proterozoic terranes and continental accretion in southwestern North America. In: *Proterozoic crustal evolution*. New York, NY: Elsevier: 1992: 459-460.
- Gundersen, L. C. S. Anomalously high radon in shear zones. In: *Symposium on radon and radon reduction technology, proceedings of a U.S. Environmental Protection Agency symposium*. Washington: USEPA: EPA/600/9-89/006a: 1989: V27-V44.
- Wanty, R. B.: Folger, P. F.: Frishman, D.: Briggs, P. H.: Day, W. C.: Poeter, E. Weathering of Pikes Peak Granite--Field, experimental, and modeling observations. In: *Volume 1, Low Temperature Environments, proceedings of the 7th International Symposium on Water-Rock Interactions, Park City, Utah*. Rotterdam: A.A. Balkema: 1992: 599-602.

Table 1. Average composition of neosome, paleosome, and Pikes Peak Granite in the Conifer, CO area.\*

Column No.	1	2	3	4	5	6
Rock type and map unit	Migmatite neosome (Xm)	Migmatite paleosome (Xm)	Migmatite paleosome (Xm)	Pikes Peak Granite (Ypp)	Pikes Peak Granite (Ypp)	Pikes Peak Granite (Ypp)
n = number of samples	Avg. (n=13)	Std. dev.	Avg. (n=6)	Std. dev.	Avg. (n=10)	Std. dev.
<b>Major oxides (wt. percent)</b>						
SiO <sub>2</sub>	73.67	2.56	52.87	7.54	73.77	1.56
Al <sub>2</sub> O <sub>3</sub>	13.71	1.36	14.95	2.67	12.75	0.47
FeTO <sub>3</sub>	1.76	1.02	8.65	1.85	2.27	1.01
MgO	0.43	0.34	6.51	4.35	0.15	0.04
CaO	1.43	1.23	9.25	4.41	0.69	0.33
Na <sub>2</sub> O	3.36	0.76	2.43	1.18	3.33	0.32
K <sub>2</sub> O	4.10	2.52	2.26	1.56	5.50	0.44
TiO <sub>2</sub>	0.11	0.05	0.70	0.17	0.19	0.11
P <sub>2</sub> O <sub>5</sub>	0.08	0.02	0.39	0.47	0.06	0.01
MnO	0.04	0.02	0.17	0.07	0.06	0.02
F	<0.01	<0.01	0.03	0.04	0.18	0.11
Cl	0.01	<0.01	0.03	0.01	0.04	0.02
LOI @ 925 °C	0.69	0.22	1.12	0.45	0.39	0.13
Total	99.32		99.34		99.24	
<b>Trace elements (parts per million)</b>						
Ba	868.72	725.83	1581.33	2801.13	354.42	216.05
Sr	297.55	172.87	688.00	987.76	51.63	17.05
Co	2.70	2.21	33.08	13.13	0.58	0.25
Ni	11.91	12.05	121.07	133.30	4.17	2.67
Cr	16.87	24.78	334.53	368.08	1.52	0.45
Cs	0.59	0.26	1.73	2.56	1.98	0.99
Hf	5.50	2.63	3.41	2.93	10.87	4.34
Rb	100.38	51.85	79.10	49.51	218.40	51.68
Sb	0.06	0.07	0.14	0.07	0.09	0.07
Ta	1.14	2.41	0.61	0.31	4.70	1.89
Zn	28.88	18.79	96.54	28.41	72.92	43.37
Zr	187.93	77.09	177.50	167.28	370.42	208.95
Sc	2.79	2.22	30.77	11.23	3.01	2.43
La	48.55	45.13	53.44	67.66	75.67	55.91
Ce	102.70	98.52	127.62	167.18	175.00	118.14
Nd	40.90	39.54	63.20	86.15	76.97	49.50
Sm	6.95	6.46	11.53	15.11	16.07	9.33
Eu	1.00	0.41	2.55	3.31	1.13	0.63
Gd	5.50	4.83	8.59	9.19	14.09	7.53
Tb	0.64	0.59	1.02	0.81	2.06	1.07
Tm	0.34	0.43	0.40	0.12	1.23	0.40
Yb	1.90	2.41	2.38	0.61	7.86	2.53
Lu	0.28	0.34	0.34	0.08	1.14	0.36
W	1.56	1.26	2.35	1.01	1.75	0.56
As	0.61	0.63	0.85	0.91	1.03	0.61
Th	36.83	24.57	11.91	12.89	34.29	13.96
U	2.86	1.25	3.37	2.55	4.78	1.59

\*Major elements by wavelength dispersive X-ray fluorescence, D. F. Siems and J. E. Taggart, analysts. Trace elements except fluorine and chlorine by instrumental neutron activation analysis, J. R. Budahn and R. E. McGregor, analysts. Fluorine and chlorine by specific ion electrode, R. A. Johnson and T. R. Peacock, analysts.

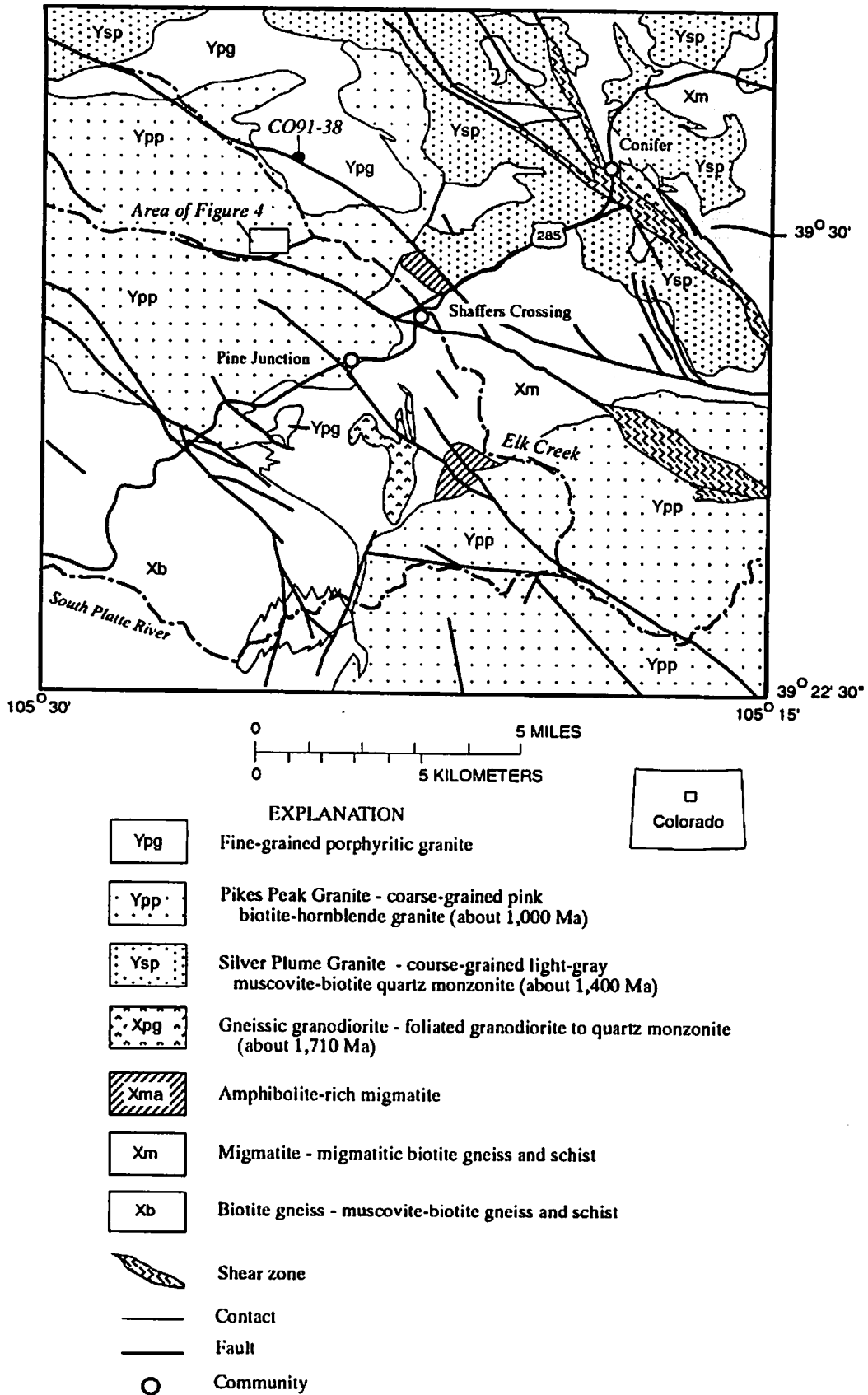


Figure 1. Geologic map of the study area near Conifer, Colorado.

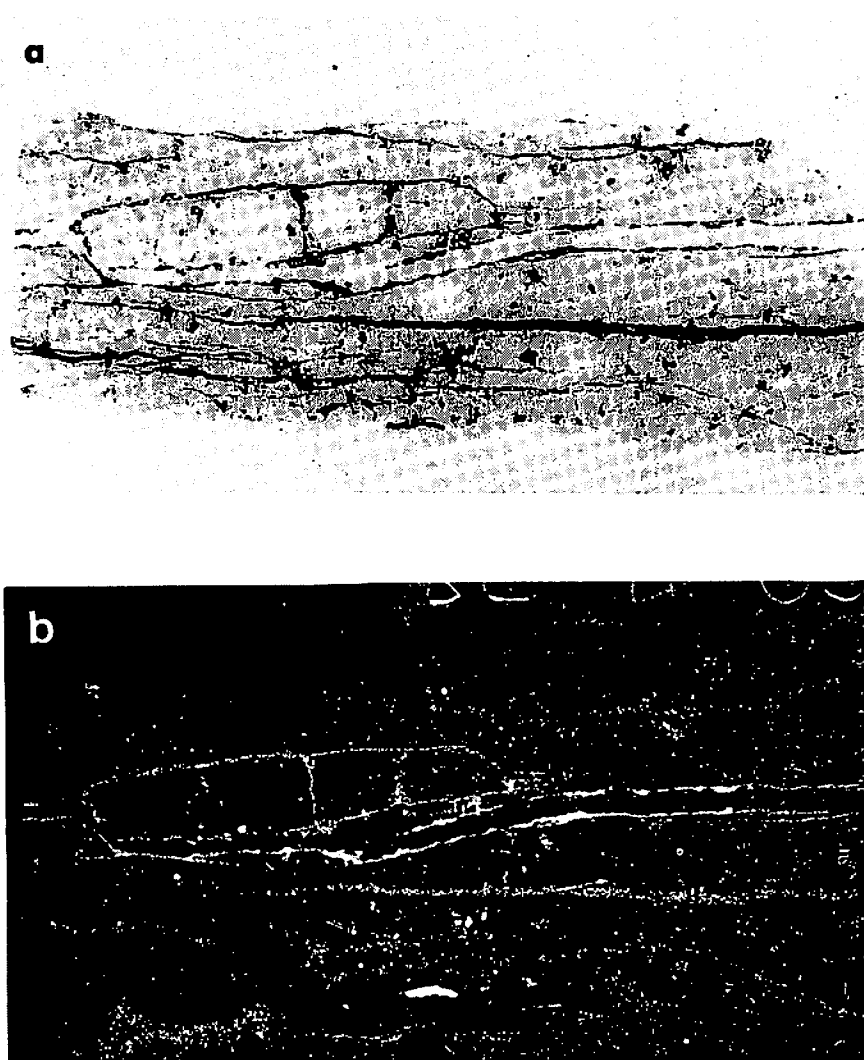


Figure 2. Photographs illustrating uranium/thorium residence in sample CO-91-38.

a--top: Photograph of a polished thin section in transmitted light. Dark lines are iron oxide coatings on fractures. The portion of the thin section shown is approximately 1.5 by 4 cm (0.6 by 1.5 in.).

b--bottom: Alpha-track map of the same thin section. The map was prepared by placing a piece of plastic sensitive to alpha particles in contact with the polished rock surface for approximately five months. After etching in hot NaOH, bubbles develop in the plastic where it has been damaged by alpha radiation. Note that the bubble trails (white lines) mimic the structure outlined by the iron oxide coated in "a" (above).



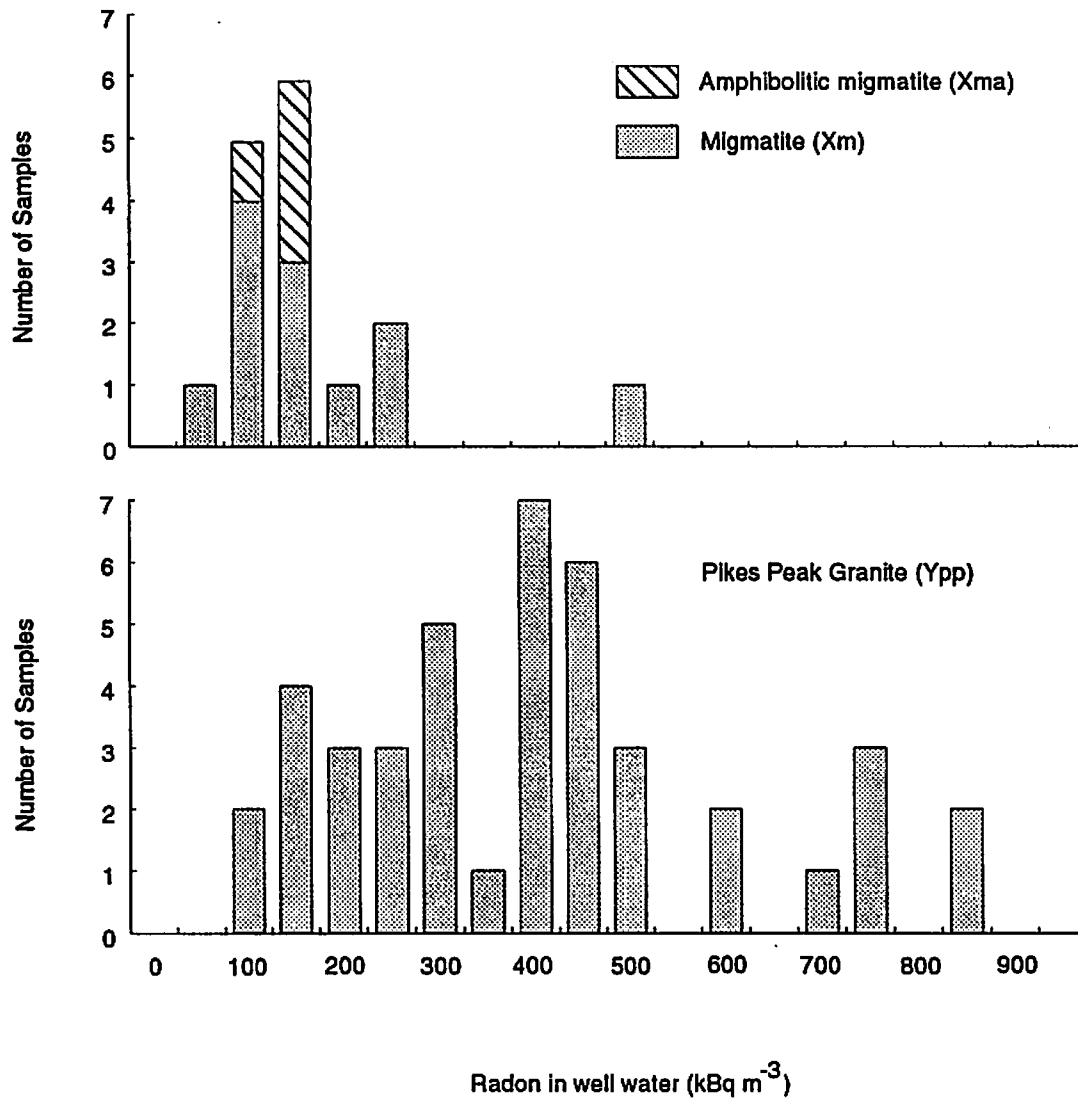


Figure 3. Radon-222 concentrations in ground-water samples from migmatitic rocks (units Xma and Xm) and Pikes Peak Granite (unit Ypp).

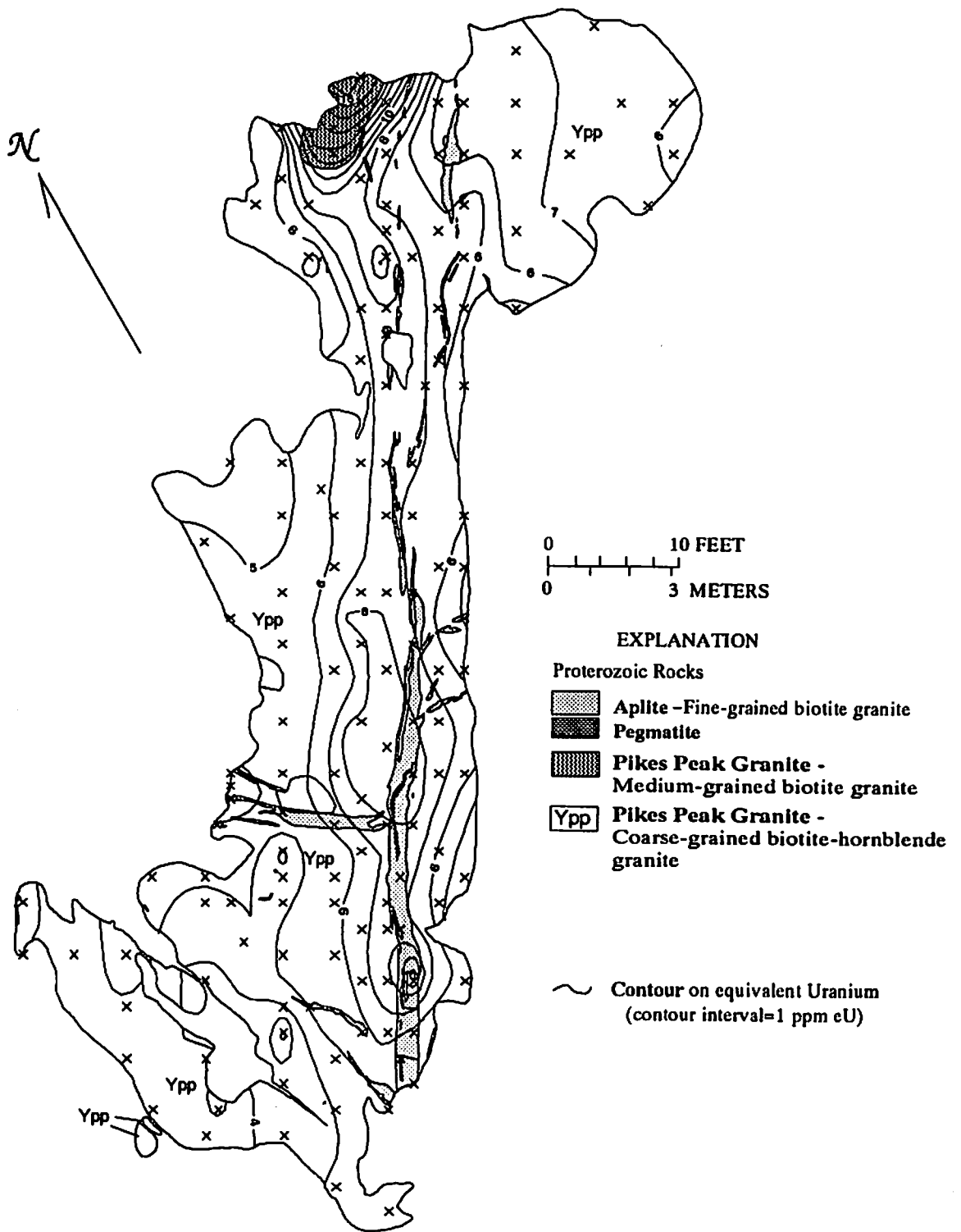


Figure 4. Geologic and equivalent uranium contour map of the Woodside subdivision outcrop.

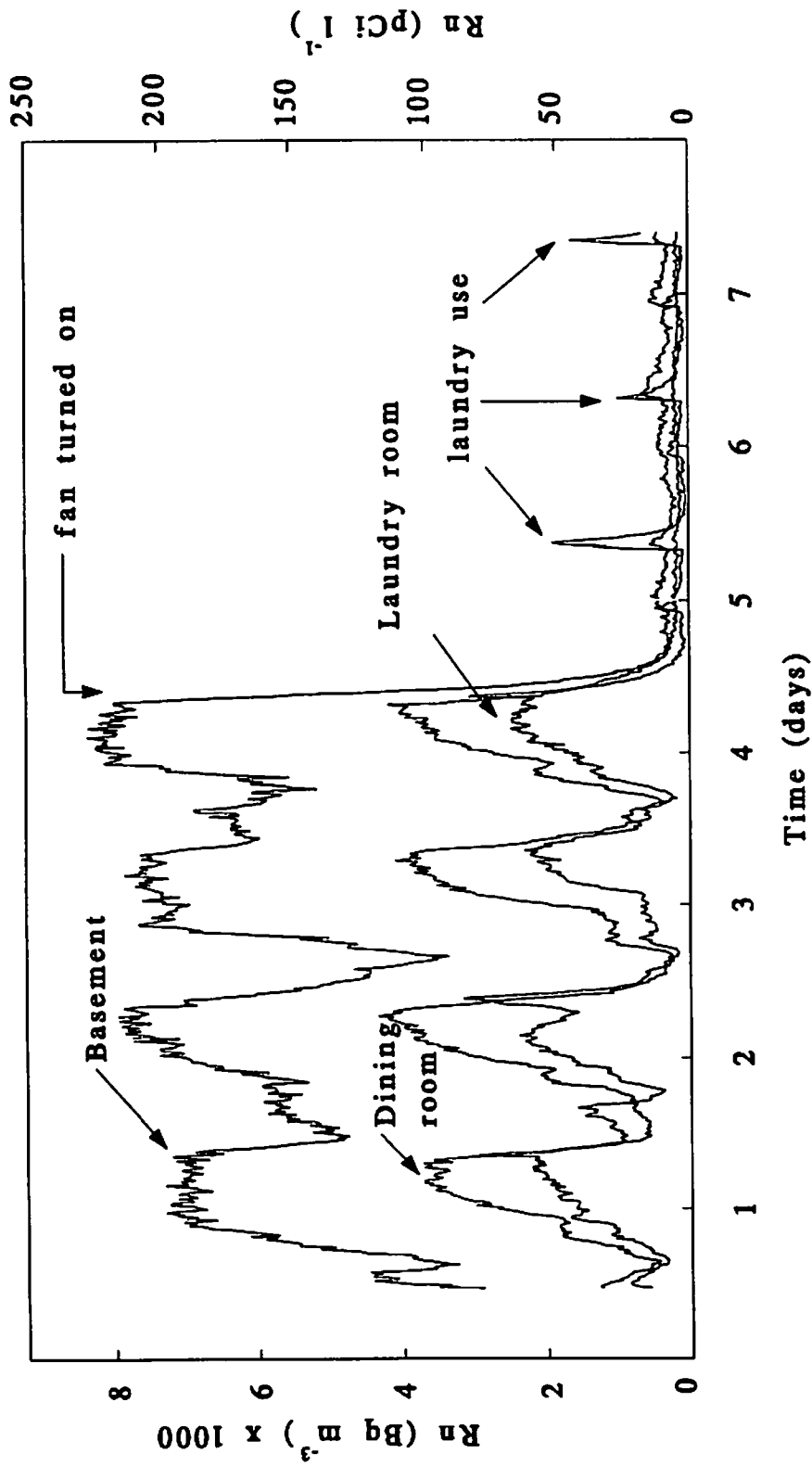


Figure 5. Indoor  $^{222}\text{Rn}$  concentrations in the basement, dining room, and laundry room before and after a high-volume fan was connected to a perimeter drain. Peaks and valleys in radon abundance before the fan was turned on at about day 4.5 are due to diurnal and other variations in soil-gas radon. Radon spikes after day 4.5 correspond to incidents of water use in the laundry room.